LTER

Principles and Standards for Measuring Primary Production

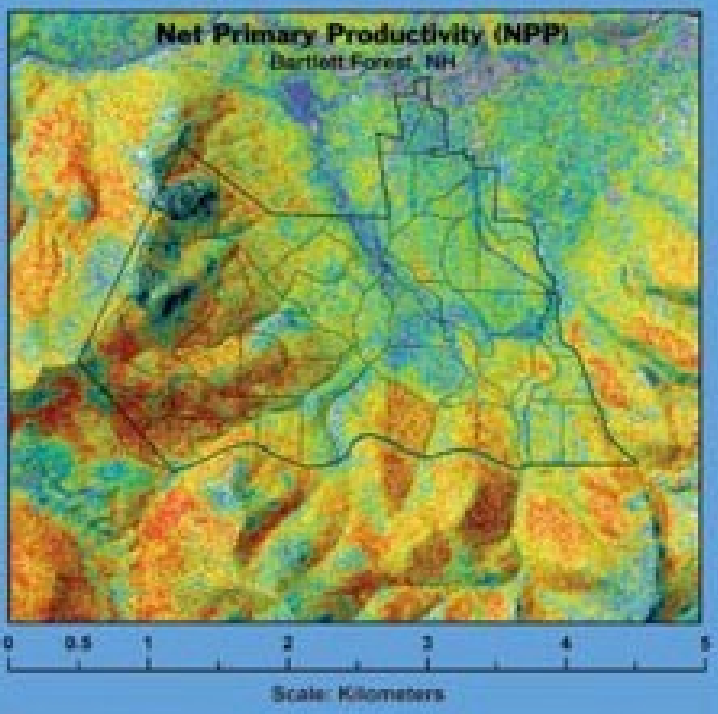

EDITED BY
Timothy J. Fahey
Alan K. Knapp

The Role of Remote Sensing in the Study of Terrestrial Net Primary Production

Scott V. Ollinger
Robert N. Treuhaft
Bobby H. Braswell
Jeanne E. Anderson
Mary E. Martin
Marie-Louise Smith

Even the most ambitious of field campaigns cover extremely small fractions of the earth's land area and capture limited samples of its ecological complexity. As a result, addressing regional-to-global environmental issues can be difficult or impossible without some means of extending field measurements to the appropriate spatial domain. Measurements that are stratified over a large number of ecological units are vital (chap. 1, this volume), but are still incomplete without knowledge pertaining to the distribution, variability, and spatial extent of each. Consequently, ecologists have become heavily invested in methods for relating observations of individual organisms and field plots to the broader regions in which they exist (e.g., Ehleringer and Field 1993; Cohen and Justice 1999).

Although a variety of scaling approaches have been investigated, there is widespread agreement that remote sensing holds a central and irreplaceable role. Remote platforms are the only means by which large and contiguous portions of the Earth's surface can be sampled, and the selective absorption and reflection of radiation by different plant tissues provide a unique basis for obtaining ecologically relevant information. However, remote observations also pose enormous methodological challenges, and to date, there is no single remote sensing method that offers an optimal approach to NPP measurement across all scales and for all research objectives. In this chapter, we review a number of approaches through which remote sensing data can be applied to terrestrial NPP, or some of its important constituents,

and discuss the trade-offs of various methods. Analogous approaches for marine ecosystems are described in chapter 9 of this volume. By nature, the remote sensing determination of NPP is more indirect than other terrestrial methods described in this volume, because ecosystem properties are only inferred through their interactions with electromagnetic radiation.

Given the breadth of the topic, our goal in preparing this chapter was not to provide a working manual of all NPP remote sensing methods available. Instead, we sought to summarize important overall strategies for NPP detection into a framework that involves the types of instruments used, the ecological properties they can be designed to detect, and the manner in which those properties can be translated into estimates of NPP. For example, instrument types can be broadly categorized into (1) passive sensors, which record reflected radiation that originates from a natural source (most often the sun), and (2) active sensors, which emit a known form of radiation from their own source (e.g., laser or radar) and record what is returned from the target surface. These categories can be further subdivided by the nature of the radiation they detect, the spatial resolution of the recorded measurements, the temporal frequency of sampling, the number of spectral channels detected, and the degree of spectral aggregation within each channel.

Not surprisingly, the properties of different remote sensors have direct bearing on the types of ecological variables that can be estimated and the methods by which they can be used to estimate NPP. For example, data from passive optical sensors typically indicate the degree to which solar radiation is absorbed or reflected by the Earth's surface at different wavelengths or view angles. Because plant pigments associated with photosynthesis have unique absorption properties, this type of data can be related to a range of variables associated with the greenness, or physiological capacity, of vegetation. Such variables, however, are not commensurate with NPP, and can be used to derive NPP estimates only when combined with process models or empirically derived algorithms.

Finally, although the methods we discuss are relevant to NPP studies in terrestrial ecosystems generally, our focus will be more heavily directed toward forests. Because forests represent the largest fraction of terrestrial carbon (C) storage and because they confront us with some of the most difficult technical challenges concerning detection of biomass and productivity, they have received a disproportionate amount of attention in the ecological remote sensing literature.

Vegetation Properties Using Passive Sensors

This section discusses methods in which vegetation properties that are observable using passive sensors can be combined with various models and empirical equations to estimate NPP. The approaches vary in terms of the complexity of the models used, their reliance on local field measurements, and the degree to which they can be applied to longer-term mechanisms of environmental and ecological change. Specifications of several passive sensors that are relevant to NPP are shown in table 11.1.

The simplest models used to derive NPP from remote sensing data are empirically derived productivity algorithms, which combine field-based relationships with

Table 11.1. Instrument characteristics for several passive sensors relevant to NPP

Instrument	Spectral Channels	Swath (km)	Spatial Resolution (m)	Frequency of Coverage	Notes
AVHRR	5	2400	1100	Daily global coverage	Continuous data since 1981
MODIS	36	2330	250–1000	Global coverage every 1–2 days	Algorithms developed for NPP prediction
Landsat 7	7	185	15–30	16 days	Landsat 1 launched in 1972
SPOT	4	60	10–20	25 days	Commercial sensor
Ikonos	3	12	1–4	3 days off nadir (144 days at nadir)	High-resolution commercial sensor
Hyperion	220	7.5	30	16 days	High spectral-resolution imaging spectrometer
AVIRIS	224	2–11	4–18	Irregular	High spectral-resolution aircraft instrument

remotely sensed canopy properties that correlate strongly with rates of production. This method offers the benefit of generating productivity estimates that are constrained to known local patterns of growth, but does not consider ecological mechanisms by which estimates can be extended to broader spatial or temporal scales. Of intermediate complexity are the light-use efficiency (LUE) models, which use the remotely sensed fraction of absorbed photosynthetic radiation to estimate maximum C assimilation rates and then adjust for suboptimal climate conditions, using a series of simple climate response algorithms. These are more dynamic in that they can account for temporal variation in climate, but they focus only on current vegetation conditions and generally do not include the ecological or biogeochemical processes needed to simulate change over the course of vegetation development or longer-term environmental change. Of greatest complexity are ecosystem process models, which simulate a wider suite of ecological mechanisms, such as photosynthesis, respiration, litterfall, decomposition, and soil nutrient turnover. Their added complexity allows simulation of a greater range of environmental factors (e.g., pollution deposition, physical disturbance, climate change), often over long time scales, but this capacity comes with added demands in terms of vegetation parameters and environmental data inputs.

In the interest of simplicity, we discuss these 3 categories of remote sensing model linkages as being distinct from one another, but readers should be aware that the boundaries between them are often blurry and hybrid approaches are also available (e.g., LUE models that include mechanisms affecting long-term biogeochemical processes).

Empirically Derived Production Algorithms

The simplest NPP models are those that consist of field-based empirical relationships between NPP and canopy properties that can be estimated using remote sensing. When

such relationships are available, this approach offers a straightforward means of producing estimates that are constrained to known patterns of productivity. The resulting accuracy is dependent only on the strength of the observed trends and on the accuracy of the vegetation property estimates. The principal disadvantage is that these approaches include no mechanisms that would allow extrapolation in time or under varying environmental conditions. Most of the canopy properties that have been examined as potential scalars between plot-based measures of NPP and remote sensing based metrics can be generalized into two groups: (1) biophysical properties such as canopy biomass or leaf area index (LAI), which represent the vegetation surface area available for light absorption, and (2) biochemical variables such as chlorophyll or nitrogen (N) concentrations, which regulate the efficiency with which harvested light can be utilized for C assimilation.

Detection of Biophysical Properties Using Broadband Sensors and Vegetation Indices

Methods for detecting biophysical properties have a longer history of development and are based on the distinct optical properties of live vegetation in the visible and near-infrared (NIR) regions of the solar spectrum. Whereas leaf reflectance in the visible region is typically low, due to the radiation absorption properties of leaf pigments (cholorphyll and caratenoids), reflectance in the NIR is high because plant cell walls strongly scatter NIR energy. Early research demonstrated that this difference in visible versus NIR reflectance could be significantly related to various properties of canopy "greenness" (e.g., Tucker 1979).

The advent of broadband Earth-observing satellites, such as the Landsat thematic mapper and the advanced very high resolution spectroradiometer (AVHRR) in the 1970s and 1980s resulted in efforts to produce simple metrics that captured variation in vegetation properties across broad spatial scales. The resulting vegetation indices (VIs), based on differing canopy reflectance at various visible and NIR wavelengths, are a composite property representing canopy cover, leaf area, and canopy architecture. Except in optically dense vegetation canopies (i.e., those with high leaf biomass and LAI), VIs tend to increase in a linear manner with increasing leaf area. The use of VIs, particularly NDVI (the normalized difference vegetation index; eq. [11.1] and SR (the simple ratio; eq. [11.2]), to predict LAI, and the application of both as estimators of productivity, has been most effectively demonstrated in forest monocultures and across large moisture gradients where substantial variation in LAI or canopy cover fraction has been correlated with field productivity measurements (e.g., Vose and Allen 1988; Gower et al. 1992; Matson et al. 1994; Fassnacht and Gower 1997; Luo et al. 2004).

$$\text{NDVI} = (\text{NIR} - \text{red})/(\text{NIR} + \text{red}). \tag{11.1}$$

$$\text{SR} = \text{red}/\text{NIR} \tag{11.2}$$

Despite their advantages and widespread use, index-based methods are often challenged by factors that cause both vegetation indices and LAI to exhibit asymptotic relationships with canopy C assimilation. At high LAI, a decrease occurs in the

incremental change in both VIs and C fixation capacity associated with a rise in LAI. This pattern has been well documented and stems from the fact that, as LAI increases, the amount of radiation intercepted by additional leaf layers declines exponentially due to increased self-shading (Gower et al. 1993; Reich et al. 1999a). The result is that relationships between NDVI and LAI eventually become saturated and, at LAI values above 3 or 4, the two variables become increasingly decoupled (Turner et al. 1999). In some systems this is a minor issue, but in closed-canopy forests, which often have mean LAI values of 4 or greater, this can be a substantial limitation. In such instances, wide variation in growth can still occur, but is driven instead by variation in leaf-level physiological capacity and the efficiency with which absorbed radiation is converted into CO_2 fixation (Reich et al. 1999b; Smith et al. 2002). The saturation in the NDVI application to LAI is exactly analogous to the saturation observed in the synthetic aperture radar application to biomass, discussed in a later section.

Detection of Biochemical Properties Using High Spectral Resolution Sensors

More recently, development of methods that allow remote sensing of leaf biochemical properties offer additional means of characterizing spatial patterns in productivity and may provide a solution for areas where LAI-based approaches are most challenged. These methods make use of the more detailed spectral information provided by high-spectral-resolution sensors or imaging spectrometers (e.g., Ustin et al. 2004). An advantage of these instruments over more conventional sensors is that instead of measuring reflected radiation in a small number (typically from 1 to 6) of broad spectral bands, they record reflected radiation over hundreds of narrow and contiguous bands, often covering a spectral range from 400 to 2500 nm. Because of their enhanced spectral coverage, the data they record have been used to detect more subtle forms of ecological variation, including leaf pigments (Fuentes et al. 2001), species composition (Martin et al. 1998; Roberts et al. 1998), the fraction of photosynthetic versus nonphotosynthetic vegetation (Asner et al. 2003), and chemical constituents such as lignin and N concentrations (e.g., Martin and Aber 1997; Smith et al. 2002). At the time of this writing, there are at least a dozen aircraft-based imaging spectrometers in operation, including NASA's airborne visible and infrared imaging spectrometer (AVIRIS) and the commercial HyMap sensor, as well as one orbital sensor—NASA's Hyperion instrument, which is part of the EO-1 satellite. A principal limitation of all existing imaging spectrometers is their small spatial coverage (swath widths of approximately 2 to 10 km), a problem that may be overcome by future sensors.

The benefit of leaf biochemistry detection in studies of terrestrial productivity stems from the well-known relationship between leaf N and photosynthetic capacity in terrestrial plants (Field and Mooney 1986; Reich et al. 1999b). The relationship has its basis in the fact that foliar N is found primarily in cellular proteins and that the principal carboxylating enzyme, Rubisco, makes up a majority of total leaf protein. Evidence supporting the link between canopy N and ecosystem productivity comes from both theoretical and empirical studies. Because N is often the nutrient

most limiting to plant growth, it has been argued that natural selection should favor individuals that allocate N in an efficient manner (Hirose and Werger 1987; Hollinger 1989; Field 1991). Sellers et al. (1992) extended this argument to show that C uptake is maximized when N is allocated optimally with respect to available solar radiation. A consequence of this relationship is that it should be possible to determine whole-canopy photosynthesis by knowing the leaf N concentration at the top of the canopy (Sellers et al. 1992). Data from stand-level studies in temperate forests support this notion, having demonstrated significant relationships among NPP, canopy-level N concentrations, and rates of N mineralization in soils (Reich et al. 1997; Smith et al. 2002; Ollinger et al. 2002).

Methods for estimating canopy N using high-spectral-resolution remote sensing have been tested by a number of investigators (Zagloski et al. 1996; Martin and Aber 1997; Townsend et al. 2003), and the usefulness of an N-based approach to estimating biomass production and soil N status has been demonstrated in studies of northern temperate forests (Smith et al. 2002; Ollinger et al. 2002). These analyses combined image data from NASA's AVIRIS instrument with extensive field measurements of canopy chemistry and related ecosystem properties. Field measurements demonstrated that patterns of aboveground NPP were more closely tied to canopy N than to several other commonly measured properties, including LAI and foliar biomass.

Structural versus Biochemical Vegetation Properties and NPP

Despite the growing number of studies that point to either biochemical or biophysical vegetation properties as useful scalars for biomass production, the relative importance of structural versus biochemical sources of variability over broad spatial scales is still largely unresolved. This is partly due to the fact that individual studies tend to focus on one variable or the other, and rarely measure both over the same range of conditions. Another source of disparity lies in the different spatial scales to which various methods have historically been applied. Given the spatial limitations of imaging spectrometers, most studies of canopy biochemical properties have focused on relatively small landscape units, whereas studies carried out over broader scales necessarily look toward canopy properties predicted by broadband VIs. Future efforts to reconcile these relationships over a range of scales are greatly needed.

In absence of the field data needed to address this question directly, an interesting alternative method involves the combined application of models designed to simulate the behavior of light in forest canopies (radiative transfer models) and those designed to simulate canopy C assimilation (ecosystem process models). To investigate the potential of this approach, a pilot study was conducted using the PnET canopy photosynthesis model (Aber et al. 1995), coupled with the SAIL-PROSPECT model of canopy reflectance and leaf optics (Verhoef 1984; Jacquemoud and Baret 1990). The aim was to test the degree to which LAI versus leaf-level chemistry affects both C uptake and light reflectance over the range of climate- and forest- type conditions in the northeastern United States (using climate and vegetation

data from Ollinger et al. 1998). Vegetation parameters that are central to both models include LAI and foliar chemistry, although SAIL-PROSPECT uses area-based chlorophyll concentrations and PnET uses mass-based foliar N concentrations. For this analysis, a linear N-chlorophyll relationship was used, based on data for deciduous tree species from Yoder and Pettigrew-Crosby (1995).

The results from this exercise indicate the combined effects of foliar chlorophyll concentrations and LAI on canopy net photosynthesis and NDVI (fig. 11.1). These results are consistent with earlier studies showing that variation related to LAI tends to saturate above LAI values of 3 or 4, whereas the effect of chlorophyll does not. Nevertheless, the responsiveness to LAI at lower LAI values is apparent, and suggests that methods for simultaneous detection of both variables would be very beneficial.

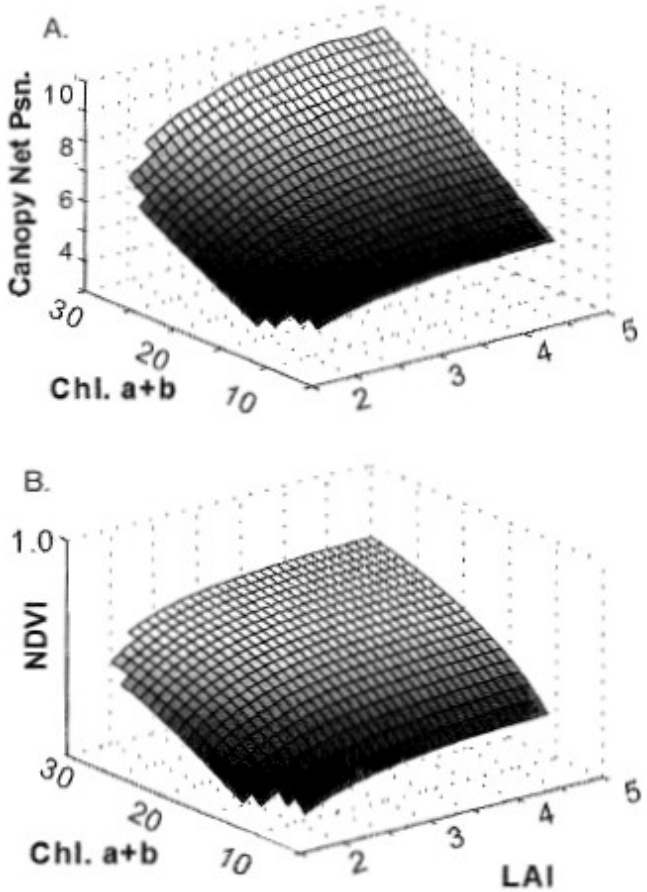

Figure 11.1. Results of simulations using the PnET and SAIL/PROSPECT models, indicating predicted responses of (A) canopy photosynthesis and (B) NDVI across the northeastern United States to variation in LAI and chlorophyll $a+b$ concentrations ($\mu g/cm^2$). Climate inputs were sampled from a GIS-based climate model over the geographic range covered by northeastern U.S. deciduous forests.

Light-Use Efficiency Models

The existence of time series of moderate resolution, multispectral reflectance data at the global scale, has enabled development of a family of techniques for estimating terrestrial productivity based on the concept of vegetation LUE. These models have evolved from the original arguments of Monteith (1972) that quantum yield of photosynthesis, the amount of C fixed per unit of incident radiation, can be used as an organizing principle for estimating overall canopy productivity. There are now a large number of efficiency models which differ in their details and complexity, but all are based on the idea that knowledge of incident radiation and the light-absorbing properties of the plant canopy can determine the maximum potential photosynthesis for that canopy. That these 2 quantities can be derived from satellite data has caused an increase in the application of LUE models, also called production efficiency models (PEM), as more remote sensing data have become available.

The first remote sensor to produce suitable large-scale data for LUE-based productivity modeling was AVHRR, which has been flown on board a series of National Oceanographic and Atmospheric Administration (NOAA) satellites from 1981 to the present, providing data at a relatively coarse spatial resolution (1 km). Since 1996, data have also been available through a commercial satellite called Systeme pour l'Observation de la Terre (SPOT), which has a radiometer (VGT) with similar properties as AVHRR but with more spectral bands, improved radiometric and geometric characteristics, and improved capacity for atmospheric correction. A recent mission led by NASA resulted in two additional satellites called Terra and Aqua, one with a morning overpass and one with an afternoon overpass. Terra and Aqua have been in orbit since 1999 and 2002, respectively, and both have an instrument called the moderate resolution imaging spectroradiometer (MODIS) that embodies similar improvements relative to AVHRR and VGT, but data are available at essentially no cost to researchers.

Monteith (1972) posited that terrestrial ecosystems are living machines whose metabolism and growth are driven primarily by the thermodynamic force of incoming solar radiation. In this framework, one needs only to consider the breakdown of efficiencies of use of this energy in order to model the individual or aggregate behavior of vegetated systems. He considered that there were seven factors, each with its associated efficiency (ε), and that the factors control all aspects governing the ratio between the amount of light incident at the top of the atmosphere and the eventual amount of fixed C. Thus, three of the factors did not relate to vegetation characteristics and are currently considered exogenous, for example, the amount of light transmitted by the atmosphere to the top of the canopy. The remaining four factors quantified the biochemical conversion and the effects of canopy structure. Most of the subsequent and current PEM approaches have been applied using coarse resolution data (1 km^2 or larger) across regional-to-global scales. These typically do not consider efficiency at the same level of detail as in Monteith's paper, primarily because of the lack of data at these scales to support the disaggregation of the canopy biochemical efficiency terms, although some recent research suggests the possibility of a unification of LUE and other approaches based on radiative transfer modeling.

Nearly all applications of PEM-type methods using satellite remote sensing data are based on the idea that the rate of C accumulation by plants (P) depends on environmental and biochemical factors in the following way:

$$P = \varepsilon * A * fAPAR * PAR, \tag{11.3}$$

where ε represents the photochemical conversion efficiency of leaves under optimal conditions (g MJ^{-1}), and A (dimensionless) represents the degree to which actual conditions are less than optimal. For example, the effects of moisture, temperature, or humidity could be represented by decomposing A into a set of scalars that decrement photosynthesis by the appropriate amount. The quantity PAR (MJ) is the amount of photosynthetically active radiation incident on the canopy. In principle, all the quantities in equation (3) can be time-varying, but the parameter that is considered to be the most central for productivity modeling is fAPAR (dimensionless), the fraction of incoming PAR absorbed by the canopy. This variable reflects the changing capacity of the canopy to harvest available light, and its potential for estimation using multispectral satellite data has driven many applications of PEMs in large-scale productivity analyses.

The principal variations and uncertainties of LUE models can be explored by discussing the four terms of equation (11.3). A given LUE-based productivity model, in a given spatial or temporal context, must assign values for conversion efficiency, environmental factors, the amount of incident PAR, and the fraction of absorbed PAR. It is conventional to think of a PEM as being driven by satellite-derived estimates of fAPAR, with the remaining terms assigned on the basis of field studies, other models, or other satellite data. Nevertheless, each of the terms carries its own assumptions, data requirements, and set of possible approaches.

The biochemical efficiency parameter ε represents the key link to plant physiology, but for the typically large spatial scale applications of PEMs (where variation in ε is poorly known), this parameter is meant to generalize extremely broadly about the behavior of leaves and canopies. In equation (11.3), P usually signifies NPP because ε is conventionally determined by observing the amount of plant dry matter accumulated over time, relative to the total intercepted light. Some recent studies use a separate model for autotrophic respiration. The meaning of equation (11.3) remains the same, except that the conversion efficiency refers to photosynthesis only, or *gross* primary productivity. Xiao et al. (2004) use the subscripted forms ε_n and ε_g to indicate this important distinction between net and gross conversion.

A persistent challenge for efficiency models in general has been the lack of understanding of factors controlling variation in ε both within and among vegetation types. Individual studies have suggested factors such as stand age, species composition, soil fertility, and foliar nutrients (Gower et al. 1999), but in the absence of a firm predictive understanding, most PEMs use either a global mean ε value for all vegetation types (Potter et al. 1993) or rely on a lookup table that assigns single values for individual biomes (Running et al. 2000). Although these approaches are satisfactory in many circumstances, measured values of ε vary considerably and, without some means of describing this variability, an important driver of C assimilation in real ecosystems remains undetected. A meta-analysis by Green

et al. (2003) offers some promise for how this challenge might be overcome. The authors compiled published values of ε and a variety of leaf and canopy-level traits from a wide array of C3 plant communities, including deciduous and evergreen tree species, and herbaceous species consisting of grasses, forbs, and legumes. Their results showed that of all factors considered, the single variable that explained the majority of the observed variation in ε was the mass-based leaf N concentration. This result suggests a potentially promising synergy between PEMs and future high spectral resolution instruments.

The estimation of fAPAR from satellite data is the central remote sensing research question associated with the development of PEMs. Shortly after the launch of AVHRR, it was shown that the pattern of differential reflectance of NIR reflectance relative to red reflectance was broadly related to field- based data on foliar biomass, LAI, NPP, and the radiometric quantity fAPAR. These relationships all follow from the fact that photosynthesis uses energy in the PAR portion of the spectrum without affecting NIR reflectance. Thus, dense plant canopies appear brighter in the NIR and darker in the visible regions than sparse canopies (fig. 11.2). This differential reflectance can be summarized with one of several indices, but the most widely used are NDVI and the SR index (equations [11.1] and [11.2]). Data from sensors that have a blue band can also be used to calculate an "atmospherically resistant" index called the enhanced vegetation index:

$$EVI = G*(NIR - Red)/(NIR + (C1 * Red - C2*Blue) + L), \qquad (11.4)$$

where the constants G, C1, C2, and L are chosen to minimize the contaminating effects of soil and atmosphere variations.

Focusing on fAPAR as the canopy biophysical parameter of interest for PEMs, there is a theoretical basis for the correlation between these indices and the amount of PAR absorbed by vegetation (Sellers 1987; Myneni and Williams 1994), but because of the complexity of the radiation regime of canopies, there is no simple analytical formula. Sellers (1987) showed that under certain assumptions that probably generally hold true (e.g., that canopies are approximately twice as optically thick in the NIR as in the visible), SR is indeed proportional to fAPAR, given a simplified model of radiation transfer. The SR index is the preferred index for some PEM models (e.g., Potter et al. 1993), but algebraically it can be shown that SR and NDVI are approximately collinear except for extremely large values of NDVI. With more complicated models of radiative transfer (e.g., Myneni and Williams 1994), a conclusion similar to those based on field studies can be reached, which is that vegetation indices and fAPAR are strongly correlated but also strongly contingent upon several other local conditions. Those conditions include the state of the atmosphere, the type and color of soil or litter, the fractional ground cover of the canopy, and the geometry of the observation. Some LUE models (e.g., Running et al. 2000) therefore use fAPAR generated by mathematical inversion of the radiative transfer models, rather than by linear transformation of SR or NDVI.

Though PEM models are generally thought of as being at least potentially global in scope, most applications have been regional. As can be seen in a review of the literature, most PEM studies have been performed on crops, rangelands, and boreal forests, a focus that may reflect the economic value of these ecosystems.

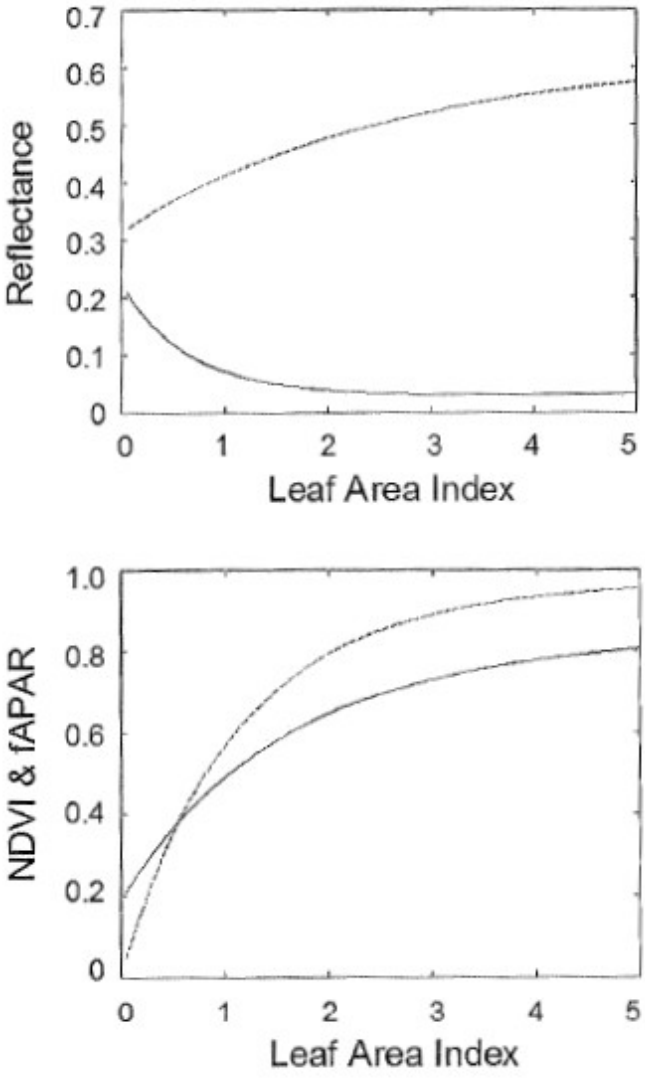

Figure 11.2. Results of a simple radiative transfer model that illustrate the underlying physical relationships that form the basis of LUE models. (Top): The differential effect of increasing leaf area index on red (solid line) and NIR (dashed line) reflectance. (Bottom): The resulting saturation curves for NDVI (solid line) and fAPAR (dashed line). It follows that NDVI and fAPAR will be approximately linearly correlated.

More recently, efforts to derive continuous NPP estimates at the global scale by combining fAPAR-based efficiency algorithms with data from the MODIS satellite have begun to take shape (Running et al. 2004; fig. 11.3). Major limitations of this approach are the relatively coarse spatial resolution (1 km), the fact that photosynthetic efficiency and foliar nutrient concentrations must be held constant within very general biome categories, and the challenge of validating predictions over such large spatial scales (e.g., Turner et al. 2003a). Nevertheless, the availability of continuous global data that can allow continuous monitoring of the NPP response to

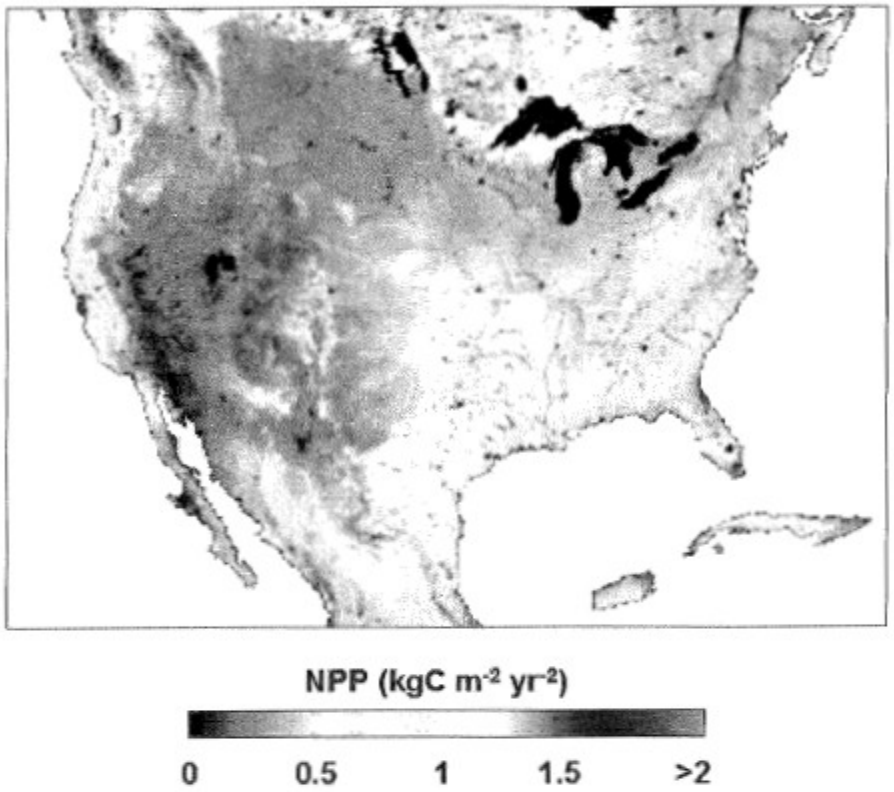

Figure 11.3. Predicted 2003 NPP over the continental United States, using an efficiency model designed to allow global monitoring of NPP with data from the MODIS satellite (Running et al. 2004).

factors that are accounted for (climate, LAI) is of obvious value for addressing a range of global-scale issues.

Ecosystem Process Models

Ecosystem process models use remote sensing primarily to initialize important vegetation input variables and then simulate ecological processes—such as photosynthesis, C allocation, respiration, litterfall, decomposition, and water balances—that affect the NPP of an ecosystem. The added complexity in these models allows them to predict a range of additional variables and to examine responses to environmental factors such as rising CO_2, atmospheric pollution, and physical disturbance. Because they are often designed to be run over longer time scales, they are more suitable for considering changes in ecosystem components such as soil C and nutrient pools that have very long turnover times.

Rather than reviewing the structure and characteristics of individual models, the focus here is on the types of input variables on which these models rely that can be obtained from remote sensing. Methods and sensors available for deriving variables mentioned in the two previous subsections will not be repeated here (e.g., use of

VIs for estimating LAI). For a more thorough review of the linkages between ecosystem process models and remote sensing, we direct readers to the review provided by Turner et al. (2004).

Vegetation Cover Type

As an initial step in parameterization, nearly all models that predict spatially distributed primary productivity in terrestrial ecosystems require some information about the vegetation or land cover type being simulated (e.g., Kimball et al. 2000; Turner et al. 2003b). Because vegetation functional classes are often adapted to specific sets of environmental conditions, they can differ greatly in terms of basic properties such as morphology, leaf life span, and C allocation patterns. Land cover classification maps provide at least a first step toward assigning appropriate values for the required parameters. Often, the challenge comes with determining how finely divided vegetation classes should be and how well remote sensing data sources can detect them.

The requirements of models in terms of specificity of vegetation classifications depends on the degree to which important parameters vary among different species and functional groups. Frequently, modelers face a trade-off between the spatial extent of a particular model application and the degree of parameter specificity that can be achieved. For instance, development of a broadly aggregated land cover map of the northeastern United States has allowed regional-scale NPP simulations to include differences in parameters such as foliar N, specific leaf weight, and leaf longevity in deciduous, evergreen, and mixed forest types (Ollinger et al. 1998). However, variation in these parameters within such broad classes can be quite large, and cannot be captured without more refined vegetation maps or independent methods of deriving these parameters directly. Additional difficulties are encountered when bringing together analyses from different regions that use different land cover classification schemes. At the global scale, efforts have been under way to reach a standardized classification for major functional types (Friedl et al. 2002), but landscape-to-regional efforts that require higher spatial resolution or greater vegetation specificity often need to derive land cover maps independently (Turner et al. 2003b).

Leaf Area Index and Canopy Height

Because LAI provides a measure of the foliar surface area available for capturing solar radiation, models that base productivity on photosynthetic rates calculated over multilayered plant canopies often require an explicit LAI input (e.g., Running and Gower 1991; Liu et al. 1999). As described earlier, LAI estimates are often derived using simple VIs, but here, too, the problem of saturation in high LAI systems is an important challenge (Turner et al. 1999). Methods that involve use of multiple VIs and multiple image collection dates offer some improvement over single VI methods (Cohen et al. 2003), and new methods involving active sensors may offer further improvement still. For example, InSAR and Lidar instruments (described in later sections) offer the benefit of sampling the vertical foliage distribution, giving them the capacity to provide detailed information on LAI as well as canopy height

(Lefsky et al. 2002a; Treuhaft et al. 2004). Hurtt et al. (2004) demonstrated the utility of this type of data by combining information on vertical structure in a Costa Rican rain forest with a height-structured vegetation model (Moorcroft et al. 2001).

Foliar N

The positive relationship between foliar N concentrations and maximum rates of net photosynthesis has been demonstrated for a large number of biomes and plant functional types, and has become a core component of a number of process-based ecosystem models (Running and Gower 1991; Comins and McMurtrie 1993; Aber et al. 1995). Spatial variation in foliar N is driven by a variety of interrelated factors, including species composition, site disturbance history, soil N, water availability, and climate (Yin 1993; Ollinger et al. 2002). Although foliar N variation is often assumed to be primarily of local importance, variation over broad spatial scales can be substantial, and is believed to be driven by the effects of climate and radiation on patterns of optimal N allocation in plants (Yin 1993; Haxeltine and Prentice 1996).

To date, only a small number of studies have made use of remotely sensed foliar N data as input for spatially distributed ecosystem models, but substantial improvements in prediction accuracy have been obtained over similar efforts where foliar N data were lacking. In one such example, Ollinger and Smith (2005) used the PnET ecosystem model to predict NPP at 18 m spatial resolution for the Bartlett Experimental Forest in north-central New Hampshire, and evaluated predictions using field measurements from a network of 39 inventory plots. When the model was run using mean foliar N values for deciduous, evergreen, and mixed forest types, agreement was reasonable in terms of the overall mean for the entire study area, but was poor on a plot-by-plot basis. When the model was run with foliar N inputs derived using the AVIRIS instrument, predictions showed a much higher degree of plot-level agreement and revealed landscape-scale spatial patterns associated with topography and forest management history (fig. 11.4).

Vegetation Properties Using Active Sensors

An active sensor transmits electromagnetic radiation, which is reflected from elements of the Earth's surface. These reflected signals travel back to the sensor, where their detection enables estimation of properties of the vegetation or ground surface. The two types of active sensors discussed in this section are radar (microwave) and lidar (optical). Although passive microwave sensors have useful sensitivities to the quantities of interest in the NPP measurement (Pampaloni 2004) with 5- to 10-km resolution, active microwave sensors provide 5- to 100-m resolution. Another advantage of active over passive sensors is that both microwave and optical active sensors enable vegetation structure measurements via received phases or time delays, as will be described below. Active measurements, however, are generally more expensive and complex, because they require transmitting as well as receiving hardware on spacecraft or aircraft.

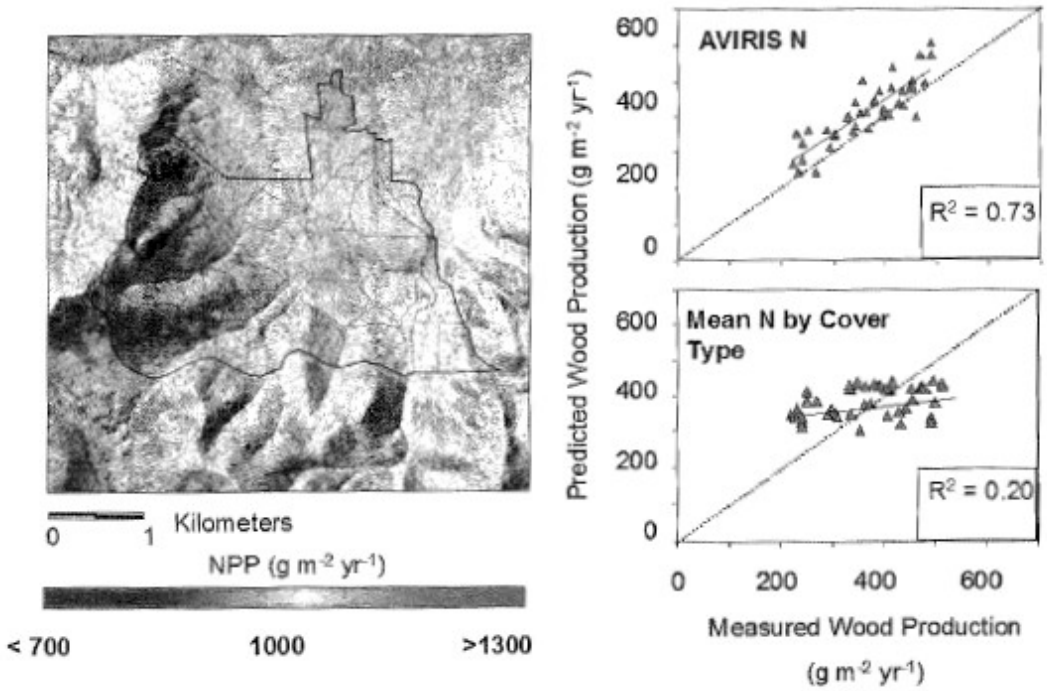

Figure 11.4. Map of predicted NPP (g m^{-2} yr^{-1}) for the Bartlett Experimental Forest, NH, generated using AVIRIS-derived foliar N as input to the PnET ecosystem model. Shadowing indicates local topography. At right are comparisons of predicted and observed wood growth, first using the AVIRIS foliar N inputs (top) and then using mean foliar N values for deciduous, evergreen, and mixed cover types (bottom). Redrawn from Ollinger and Smith (2005). (See the cover for a color version.)

Whether microwave or optical, active remote sensing detects reflections of a transmitted beam from components of a vegetated land surface. Electromagnetic reflections arise whenever there is a discontinuity in a key electromagnetic property called the "dielectric constant." The dielectric constant of an object—a leaf, branch, trunk, or the ground—depends on its chemical composition. Its square root is inversely proportional to the speed with which an electromagnetic wave propagates in the medium, and directly proportional to how much of it is absorbed. Vegetation and ground surfaces reflect because their dielectric constants are higher than that of air, creating dielectric discontinuities at their surfaces. Figure 11.5 shows schematically that the signal reflected back to an active sensor depends on both the strength and the number of the discontinuities as well as on the organization of the reflecting objects in the scene. That is, it depends on what the objects are, how many there are, and where they are. The following subsections describe two conceptual ways in which radar and lidar sensors can contribute to estimating NPP in ecosystems (1) by determining biomass at multiple time periods and thereby estimating a biomass change rate (multiple-epoch biomass method), and (2) by determining other properties of the vegetation which, when combined with empirical production algorithms or process models, such as those described earlier, directly correlate with NPP (direct NPP correlate method).

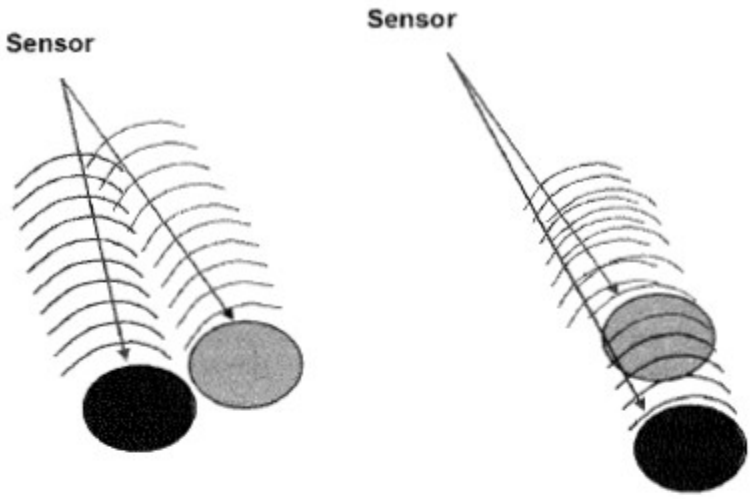

Figure 11.5. A schematic demonstration indicating that (Left) a strong reflection from the dark object, indicated by dark black wavefront lines, and a weaker one from the light object have an additive effect on the signal detected at the sensor. (Right) With the same 2 reflecting objects, the signal from the dark object is attenuated if it is vertically behind the light object. The total received signal will be weaker than that of the left portion of the figure, though the reflecting objects are the same; only their spatial locations have changed.

Radar Measurements: Biomass and Its Accumulation over Time

The application of radar to estimates of NPP is in its infancy. Nevertheless, given the direct relevance of radar sensors to measurements of vegetation biomass, a review of the prospects for estimating NPP with products currently derived from radar is warranted. There are two types of radar that potentially can be applied to NPP measurements (fig. 11.6): (1) synthetic aperture radar (SAR) and (2) interferometric synthetic aperture radar (InSAR). SAR is primarily sensitive to the amount of vegetation in a scene, and InSAR is primarily sensitive to the vertical distribution of the vegetation.

Before proceeding, it should be stressed that vegetation biomass, biomass accumulation, and NPP are three distinct properties, and relationships among them vary over time and between ecosystems. Hence, the ability to detect biomass or its accumulation over time does not translate directly to an ability to estimate NPP. The relationship between NPP and biomass accumulation on a vegetated land surface can be generalized as follows:

$$\begin{aligned} \text{NPP} = {} & \text{Increase in standing biomass} \\ & + \text{Biomass lost to mortality and litter production,} \end{aligned} \tag{11.5}$$

where the contributions of herbivory and C exudates are ignored. In young systems dominated by perennial vegetation, biomass accumulation can represent a large fraction of NPP because growth rates tend to be considerably higher than death rates. In maturing systems, however, biomass accumulation declines and typically

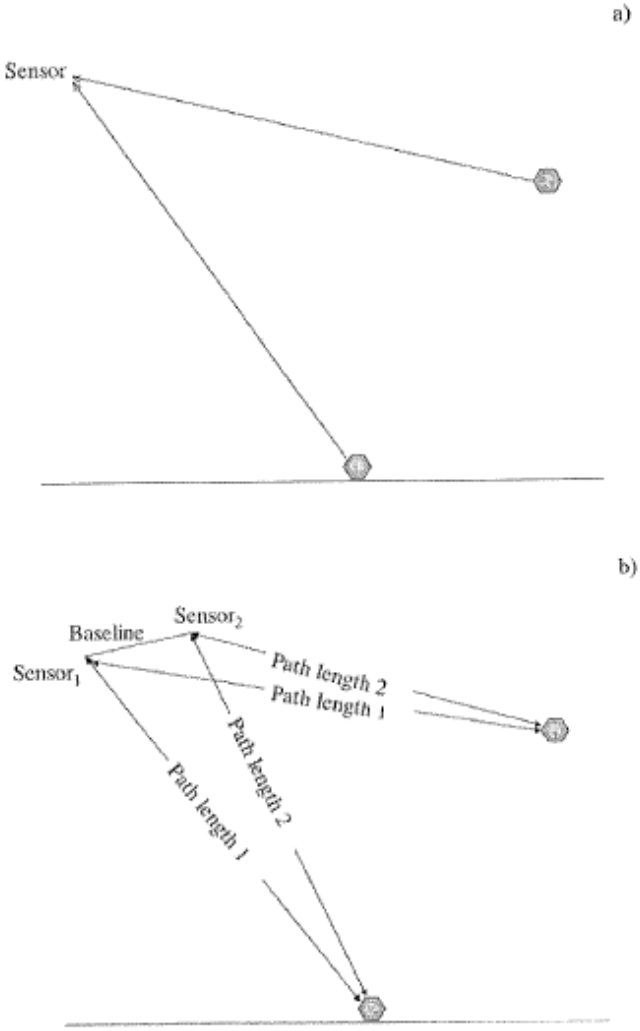

Figure 11.6. (Top): SAR uses 1 sensor to receive power reflected back to it by 2 green schematic vegetation components. SAR is sensitive to the powers induced by the components, but not to their location. (Bottom): InSAR uses 2 sensors and is sensitive to the powers as well as the vertical location of the scatterers via the differences in path length of each component to the 2 sensors.

becomes small with respect to NPP, due to increasing rates of both mortality and litterfall. In systems dominated by annual grasses and herbs, changes in biomass can be equal to NPP over seasonal time scales, but independent of NPP when viewed over multiple years. Despite the variability in NPP-biomass relationships, most NPP estimation methods require knowledge of biomass at some stage of their application. Hence, methods of direct biomass detection are often beneficial, particularly where estimates of other important properties are available. This section discusses how biomass measurements are made with radar and the prospects of using multiple-epoch measurements to estimate a rate useful to NPP determination.

Biomass from SAR

Qualitatively, SAR measures the power of the returning signal due to vegetation using a single sensor (fig. 11.6a). SAR is directly sensitive only to the strength and number of the dielectric discontinuities, as suggested by figures 11.5 and 11.6. While SAR is affected by the location of components of reflecting surfaces—the signal at the sensor in figure 11.5 (right) is weaker than that of 11.5 (left)—SAR cannot tell the difference between changes in location and changes in component strength and number. In figure 11.6a, the received signal is independent of the vertical position of the 2 schematic vegetation elements shown.

For microwave radiation, the dielectric discontinuities depend principally on the water content of the vegetation or the ground surface. More discontinuities mean, for example, more foliage, which in turn can mean more biomass. SAR estimations of biomass (e.g., Dobson et al. 1995; Paloscia et al. 1999; Santos et al. 2003) assume that more power means more biomass. The biomass estimation procedure starts with the following general, often empirical, relationship between biomass and SAR powers:

$$f(biomass) = g(SAR\ power_1, SAR\ power_2 \ldots SAR\ power_N, parameters_{1 \ldots M}) \quad (11.6)$$

where f is some function of the biomass and g is another function of SAR powers 1 through N and parameters 1 through M. The parameters must be determined by test plots, and then applied to other plots to estimate biomass, using equation (11.6). The internal consistency of equation (11.6) for a single set of plots is also used to demonstrate biomass estimation and gauge its error.

The different SAR powers in equation (6) arise from differences in polarization (Marion 1965) and frequency. Using SAR of different polarizations improves vegetation and surface characterization if there are "oriented" objects, such as the ground (Papathanassiou and Cloude 2001). Generally, lower frequencies (e.g., P-band at 80 cm wavelength) penetrate further into vegetation and scatter from larger objects than higher frequencies (C-band at 6 cm wavelength and X-band at 3-cm wavelength). Spaceborne demonstrations of biomass estimation have used JERS (Japanese Earth Resources Satellite, L-band, 25 cm), ERS (European Remote Sensing, C-band), RadarSAT (C-band), and SIR-C (Shuttle Imaging Radar, L-, C-, X-band).

Assigning a single accuracy to biomass estimation with SAR is difficult because virtually every study uses different forms of f and g in equation (6), and different numbers of parameters and input SAR powers. Forest biomass typically falls within the range of 0–700 Mg/ha, and is often less than 300 Mg/ha, except for tropical and old-growth forests, which populate the high end of the range. Average errors with 1–3 parameters in equation (6) have been reported in the 30% range with JERS-1 (Luckman et al. 1998). Some experiments which sort results by species, structure, or other metrics using more ground data show errors of less than 10% with SIR-C (Dobson et al. 1995). Many reports say that the estimation error may be due in large part to field measurement error, in which case the intrinsic radar error might be much

smaller than the above. This hypothesis has yet to be carefully tested for SAR experiments.

Virtually all experiments agree with the implications of figure 11.5 regarding the ambiguity introduced by vegetation structure (e.g., Imhoff 1995). Although SAR powers respond to vegetation vertical structure, they cannot be used to uniquely specify the structure. A lack of knowledge regarding structure induces errors in the conversion of radar observations to biomass, as in equation (6). Figure 11.5, for example, would be interpreted as two different biomasses, though only the vertical organization of the vegetation differs between the figures.

Two salient features are used to describe biomass estimation accuracy, the location of the "saturation point," where the curve flattens out, and the scatter about a smooth trend (fig. 11.7, top). The saturation point generally occurs at lower biomasses for higher frequencies. The scatter indicates the biomass error. In the figure, below 100 Mg/ha, for example, scatters indicate that an approximate range of 10–20 Mg/ha of biomass, 20–40% of the biomass, could correspond to a single radar power.

Biomass from InSAR

InSAR utilizes two receivers to view the vegetation from two different perspectives (fig. 11.6b). In addition to being sensitive to the reflecting strength and the number of vegetation components, InSAR is directly sensitive to the altitudes of the components of the vegetation above the ground surface via the path length difference from each component to the two sensors (Treuhaft et al. 1996). A single InSAR observation yields an InSAR phase, proportional to the average height of the vegetated surface, and an InSAR coherence, which decreases as the vegetation becomes more vertically distributed (Treuhaft et al. 2004). If one receiver is flown by a site at two different positions, a repeat-track baseline is formed. If there are two real receivers, an instantaneous baseline is formed. Biomass estimation has been reported a few times using repeat-track, spaceborne baselines of ERS and JERS-1 (Luckman et al. 2000; Santoro et al. 2002; Askne et al. 2003; Pulliainen et al. 2003; Wagner et al. 2003). The repeat-track studies, which derive their sensitivity to vegetation volumes from the changes in the scene during the observation epochs, generally show that C-band InSAR is much more useful for biomass estimation than C-band SAR. This conclusion is further supported for fixed-baseline InSAR by a simple model calculation (Treuhaft and Siqueira 2004). ERS repeat-track InSAR passes generally outperform JERS-1 because 1-day repeats could be obtained with the ERS-1 and ERS-2 satellites, whereas JERS repeated in 45 days. With longer repeat times, the degree of decrease in coherence no longer discriminates between different volumes of the forest, as it does for 1-day repeats (Askne et al. 2003), owing to excessive coherence loss induced by scene changes between repeat tracks. For frozen boreal forests, Santoro et al. (2002) and Askne et al. (2003) report the best biomass estimation precision using repeat-track InSAR coherence from ERS-1 and ERS-2 of about 25% on 2–20-ha stands of up to about 200 Mg/ha.

Biomass estimation has been reported only once, using instantaneous baselines from the airborne AirSAR (Treuhaft et al. 2003). In the instantaneous baseline

experiment, the phases and coherences from six C-band baselines were used to estimate the vertical profile of leaf area density (LAD) for stands predominantly of ponderosa pine, grand fir, and larch in the Metolius River basin in central Oregon. Multiple baselines are required to estimate vertical profiles (Treuhaft et al. 2002) and, generally, multiple baseline, multiple polarization (Papathanassiou and Cloude 2001), multiple frequency, or ancillary information (Treuhaft et al. 1996; KelIndorfer et al. 2004) is required to quantitatively estimate vertical characteristics of forests. The profiles estimated in the multiple-baseline biomass experiment were normalized by LAIs estimated from airborne hyperspectral data from AVIRIS. Unlike equation (11.6) or the repeat-track InSAR experiments, biomass was correlated with structural variables estimated from the remote sensing rather than raw observations. Specifically, figure 11.7 (bottom) shows field biomass versus remote sensing biomass, calculated as

$$biomass = \mathrm{a} + \mathrm{b}\,(\mathrm{LAI}^{*}\sigma_{LAD} + \langle z \rangle_{LAD}), \tag{11.7}$$

where LAI is the leaf area index from hyperspectral data, σ_{LAD} is the standard deviation of the LAD distribution from InSAR, $\langle z \rangle_{LAD}$ is the LAD-averaged vegetation height from InSAR, and a and b are best-fit parameters. The scatter of the remote sensing about the field measurements was 25 Mg/ha, or about 16% of the average biomass of the 1-ha stands. Note that biomass reported from C-band SAR power saturates at about 50 Mg/ha (Imhoff 1995), but there is little evidence of saturation based on C-band InSAR (fig. 11.7, bottom). This further suggests that InSAR saturation characteristics are more favorable than those of SAR for biomass estimation. Furthermore, the accuracy indicated by the scatter of figure 11.7 (bottom) is better than most two-parameter determinations from radar power, and is about the same as the best lidar determinations (e.g., Drake et al. 2002). Additionally, Treuhaft et al. (2003) estimate about a 15% error in the field biomass measurements, possibly implying very high performance for the remote sensing technique. As noted above, an experiment in which the field errors were reduced substantially would have to be conducted to claim much higher accuracy for InSAR-based remote sensing.

Though the results of figure 11.7 (bottom) are significant with 99.5% confidence, they are the first of their kind, sample only one conifer forest, are based on only 11 stands, and must be regarded as a suggestion of the potential of InSAR-determined, structure-based biomass, rather than a demonstration of reliable performance. Extensive tests of the InSAR-profiling approach in other vegetation types are needed. Although virtually every study using radar power to estimate biomass cites unknown structure ambiguities (e.g., fig. 11.5), studies in which estimated InSAR structure is used to interpret and correct radar power estimation have yet to be done.

Multiple-Epoch Biomass Estimates

In young, rapidly aggrading ecosystems, where the accumulation of biomass over time represents an important fraction of NPP, radar-based biomass estimates have a clear application when acquired over two or more time periods. In more mature

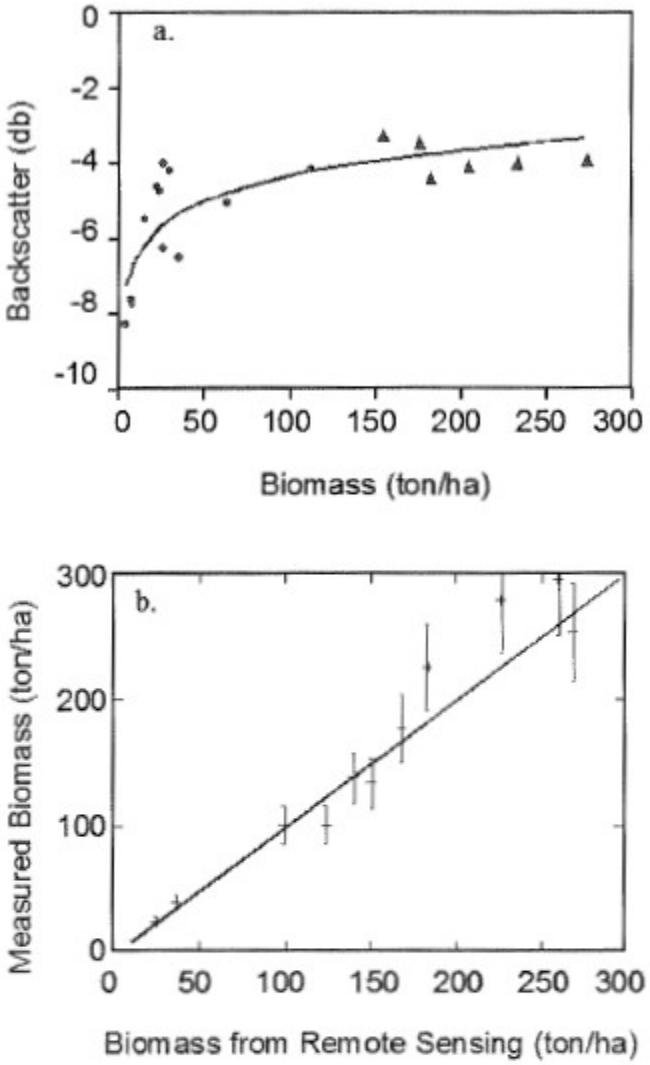

Figure 11.7. (Top): Radar P-band backscatter power versus field biomass in tropical forest stands of 0.1–0.25 ha, showing typical increases of power with biomass and a flattening out or saturation of power versus biomass at higher biomasses. Triangles are primary forest, and circles are secondary succession. The line is the function indicated. Redrawn from Santos et al. (2003). (Bottom): Biomass from C-band InSAR and hyperspectral remote sensing versus field biomass for 11 stands of ponderosa pine, grand fir, and larch in central Oregon. Relative vertical leaf area density profiles were estimated from multiple-baseline InSAR using AirSAR and normalized by a leaf area index from AVIRIS hyperspectral data. The line is y = x. Redrawn from Treuhaft et al. 2003.

systems, as standing biomass reaches its maximum, biomass accumulation declines toward zero, and the importance of combining biomass estimates with measurements of ingrowth, mortality, and litter production becomes paramount. In the maturing forests of eastern North America, for example, the incremental change in biomass is often less than 10% of NPP on an annual basis, and is an even smaller

fraction of the standing biomass observed at any one time. In such cases, biomass must be remotely sensed with a few percent accuracy in any one year to contribute meaningfully to NPP determination using multiyear estimates. This can plausibly be accomplished with repeated measurements using InSAR and to a lesser degree with SAR. Multiple InSAR coherence-based experiments have yielded approximately 13% accuracy in biomass retrieval over boreal forests (Santoro et al. 2002), whereas Salas et al. (2002) suggested that repeated SAR measurements yielded accuracies at the 30% level. Higher accuracies could also be accomplished with fewer measurements if the fundamental performances of the SAR and InSAR approaches were improved. Quantifying the accuracy of the field measurements themselves will also be important to further the assessment of radar-based methods.

Virtually all radar biomass demonstrations that could be used in the multiple-epoch method measure aboveground biomass. Belowground NPP can be equal to 20%–50% of the aboveground NPP (Gower et al. 1992; Fahey et al. 2005). Therefore, to date, radar biomass measurements can be used only for the aboveground component of NPP, rather than the total NPP. The degree to which aboveground biomass rate can be reliably correlated with belowground biomass must be investigated, perhaps along with structural correlates from InSAR and lidar.

Biomass accumulation estimates using radar-based approaches are also possible in grasslands, crops, and herbaceous communities, although measurements are required over seasonal, rather than annual, time scales. In one example, Moreau and Le Toan (2003) show approximately 30%–50% biomass estimation accuracy for water-saturated grasslands observed at C-band with ERS. Ferrazzoli et al. (1997) obtained an accuracy of about 50% in the estimation of aboveground crop biomass using P-, L-, and C-band AirSAR over plots containing corn, sunflowers, sorghum, and wheat. These accuracies should translate to NPP accuracies of about the same order, but a correlative analysis of aboveground and belowground NPP would indicate the performance for the larger belowground component. Furthermore, observed accuracies depend somewhat on the availability of a so-called ground bounce due to the water in the ground. The task of correcting for standing dead tissues represents an additional challenge, though one which may be minimized in systems that are annually burned or harvested.

Radar Measurements: Direct NPP Correlates

This section outlines the potential for estimating biophysical quantities from radar observations which correlate directly with rates of NPP. This link could be achieved through use of empirical algorithms or via process models. Because there are few examples of this approach in the literature, the discussion will be brief. As mentioned above, SAR correlates primarily with the amount of material, or the aboveground biomass, in a vegetated land surface. Under some circumstances, the biomass itself, rather than the biomass change between two or more time periods, could be considered as an NPP correlate. Across biomes, there is a coarse relationship between biomass and aboveground NPP (Webb et al. 1983). Within biomes, however, wide variation around this trend can be expected from factors such as stand age, species composition, disturbance history, and edaphic properties. Biomass from

SIR-C/X-SAR has been used with an allometric model of aboveground NPP (Bergen and Dobson 1999), but many additional field constraints were required. It is possible that with adequate ancillary information and sufficient diversity in frequency and polarization, this approach could represent a useful complement to other NPP detection methods.

Structural properties retrieved from InSAR are affected by factors such as species composition, stem density, stand age, and vegetation height, all of which relate to NPP in some way or another (Waring and Running 1998; Mencuccini and Grace 1996; Kicklighter et al. 1999; Smith et al. 1999). As an example, secondary forests that are in an early state of regrowth following harvesting contain less biomass, but are often more productive than more mature forests (Pregitzer and Euskirchen 2004). Hence, their vertical structure as measured by InSAR may well be useful as a correlate with NPP, although here, too, information regarding other properties of the sites and vegetation conditions would likely be required. The optimal means of direct-correlate estimation from InSAR and other techniques, perhaps combined with climate inputs that can also be derived from remote sensing (e.g., Running et al. 2004), are subjects for future research.

Lidar Measurements

Laser altimetry, (or lidar, light detection and ranging) is an emerging remote sensing technology with a variety of applications of interest to terrestrial ecologists (Lim et al. 2003; Dubayah and Drake 2000; Wehr and Lohr 1999; Lefsky et al. 2001, 2002a). Lidar-derived metrics have proven effective for predicting ecological variables such as canopy height and structure, the density of forest cover, biomass, and light transmittance (Drake et al. 2002; Lefsky et al. 2002a; Means et al. 1999; Harding et al. 2001; Parker et al. 2001). In particular, the demonstrated capability of lidar to characterize the amount of standing biomass in an ecosystem provides a strong foundation for determining rates of primary productivity (but note the previous discussion on distinctions and relationships between biomass and productivity). After a description of the lidar measurement, the multiple-epoch biomass method from lidar data will be followed by the direct NPP correlate method, just as in the radar section.

The Lidar Measurement

The basic measurement made by a lidar device is the distance between the sensor and the target, obtained by an accurate measurement of the time elapsed between a pulsed signal emission and the return signal. Lidar instruments currently in use can be described as either *discrete return* or *full waveform* lidar (Lim et al. 2003). Discrete return lidar instruments measure a single (or a few) vertical distance(s) within the lidar footprint, often the first and last signal returns. Discrete return lidar instruments typically operate at a high spatial frequency, with a small footprint, and are optimized to provide detailed information on ground elevation and canopy surface. In contrast, waveform recording lidar instruments record the time-varying intensity of the return signal, and thereby yield an increased amount of information

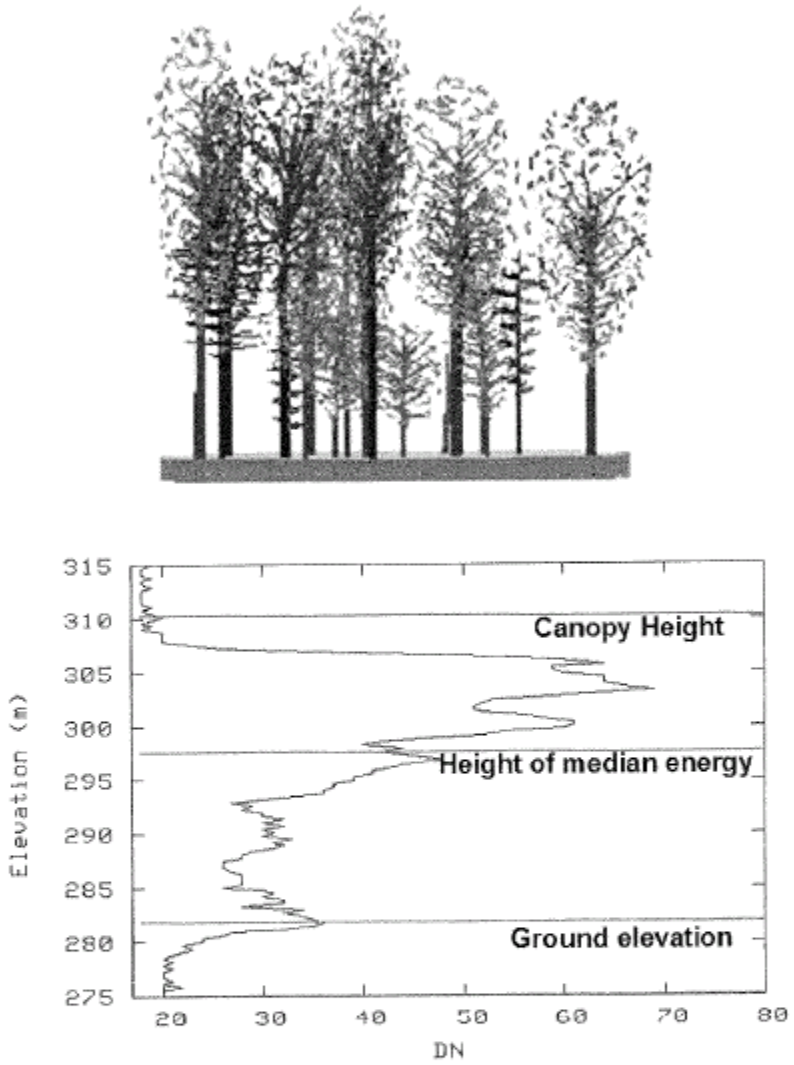

Figure 11.8. Full waveform lidar example. (Top): Canopy simulation derived from field measurements. (Bottom): Waveform data corresponding to the canopy depicted at top, indicating the fully digitized waveform data and ground elevation, top of canopy, and height of median energy in the return signal. Data from a 2003 LVIS flight over the Bartlett Experimental Forest, Bartlett, NH.

aboveground biomass can be explained by lidar metrics (Lefsky et al. 1999a, 1999b, 2005a; Means et al. 1999; Nilsson 1996; Drake et al. 2002). These studies have been conducted in a number of different biomes, including temperate deciduous, temperate coniferous, tropical wet forest, and boreal coniferous biomes. In addition, Lefsky et al. (2002b, 2005b) and Drake et al. (2003) have begun exploring the generality of relationships between lidar metrics and allometric estimates of above-ground biomass across contrasting biomes and among sites of different productivities within

a biome. Further investigations of these cross- and within-biome relationships will play a significant role in scaling from small-scale airborne lidar estimates of biomass to large-scale estimates from future spaceborne lidar instruments.

To date, few spatially coincident lidar data sets have been collected over multiple time periods. In a space-for-time substitution, Lefsky et al. (2005a) described a spatially extensive approach to estimating the woody component of aboveground NPP (NPP_w) based on deriving stand age and biomass in landscapes subject to stand-replacing disturbance regimes from Landsat and lidar data products. Stand age is derived by iterative unsupervised classification of a multitemporal sequence of images from a passive optical sensor (e.g., Landsat TM). Stand age is then cross-tabulated with estimates of stand height and aboveground biomass from lidar remote sensing. NPP_w is calculated as the average increment in lidar-estimated biomass over the time period determined, using change detection. This approach compared well with forest inventory estimates, but contrasted significantly with estimates derived from a spatially distributed biogeochemistry model (Lefsky et al. 2005a).

Model Parameters and NPP Correlates from Lidar Observations

A second approach uses lidar metrics as input data to ecosystem models that estimate NPP. Modeling studies have demonstrated the utility of lidar data in the production of input parameters such as tree height and vertical foliage distribution, which more accurately define current canopy conditions and relate directly to rates of productivity. Kotchenova et al. (2004) demonstrated the use of waveform lidar in modeling gross primary production (GPP) of deciduous forests. They parameterized a photosynthesis model using standard sunlit/shaded leaf separation (two-leaf) and multiple layer approaches. Model simulations using a uniform leaf distribution versus a vertical leaf distribution derived from waveform lidar resulted in large differences in the calculated GPP values, and demonstrated the importance of vertical canopy structure in determining both the distribution of direct and diffuse light within the canopy and the distribution of sunlit and shaded leaves. Hurtt et al. (2004) combined lidar-derived canopy height with a height-structured terrestrial ecosystem model called the ecosystem demography model (ED; Moorcroft et al. 2001). The use of lidar-derived height in this model allowed the model to be initialized with actual vegetation structure, in contrast to potential vegetation conditions, thereby accounting for the effects of land use history and disturbance on standing biomass and C flux.

Collectively, these recent studies combine to illustrate the potential utility of developing lidar technologies to improve estimates of aboveground biomass. Although lidar, like other remote sensing instrumentation, cannot directly measure NPP, the ability to measure vegetation structural attributes, aboveground biomass, and change in biomass over time from airborne and/or spaceborne platforms should help to increase our understanding of trends in NPP at local and regional scales.

Concluding Remarks

In reviewing approaches for applying remote sensing to the study of terrestrial NPP, it should be clear that a wide variety of methods exists, and each has its own set of inherent strengths and limitations relative to factors such as spatial scale and resolution, frequency of data collection, the nature of the ecological properties that can be captured, and the ability to examine the influence of changing environmental conditions. Methods that rely on broadband vegetation indices, for example, can be applied at regular intervals over continental spatial scales, given the large scene size and regular orbits of sensors such as MODIS and AVHRR. However, their coarse spatial resolution (often ~1 km) and limited spectral detail often don't provide the detail needed to capture fine-scale features of interest to researchers and managers working at subregional scales. Methods involving imaging spectroscopy or active sensors may account for finer-scale variation related to additional vegetation attributes (e.g., biomass or biochemistry), but presently cover smaller portions of the Earth's surface or do not collect data at frequent intervals.

Despite these differences, a common feature of all remote sensing methods is their ability to increase dramatically the amount of land surface that can be sampled, often providing spatially contiguous information at multiple periods in time. As such, remote sensing provides a complement to field measurements by filling gaps between measurements at individual locations and specific points in time. Because nearly all remote sensing methods are in some way or another built up from ground-level measurements—be they measurements of leaf physiology, canopy-light interactions, or stand productivity—remote sensing should be seen as an extension of other methods, rather than divorced from them.

An aspect of remote sensing that is beyond the scope of this chapter, but worth mentioning nonetheless, is the potential to use remotely sensed spatial patterns as a means of examining underlying controls on ecosystem productivity. Whereas field plots typically capture limited samples of the environmental conditions in which ecosystems exist, the large sample sizes provided by remote sensing instruments allow NPP estimates to be contrasted with spatial and/or temporal patterns of important variables, such as climate, topography, and soil properties. Extensive data for variables such as these often exist in the form of geographic information systems or climatological databases, and can be used to shed light on mechanisms controlling variation in NPP (e.g., Braswell et al. 1997). Analyses of this nature should open the minds of researchers to the potential role of remote sensing in basic ecological research.

Acknowledgments This work was supported by NASA through grants from the Terrestrial Ecology Division's Carbon Cycle Sciences Program (CARBON/0000-0243 and CARBON/04-0120-0011), the Interdisciplinary Science Program (NASA IDS/03-0000-0145), and the Earth System Science Fellowship Program (NGT5-30481. We also received support from the U.S. Department of Energy's National Institute of Global Environmental Change (NIGEC grants DE-FC02-03ER63613 and DE-FC03-90ER61010) and the USDA Forest Service Northeastern Research Station. Portions of this research were carried out at the Jet Propulsion Laboratory, California Institute of Technology, under a contract with the

National Aeronautics and Space Administration. We received helpful assistance from Lucie Plourde and Julian Jenkins, and we thank Steve Running for providing us with the image shown in figure 11.3.

References

Aber, J. D., S. V. Ollinger, C. A. Federer, P. B. Reich, M. L. Goulden, D. W. Kicklighter, J. M. Melillo, and R. G. Lathrop, Jr. 1995. Predicting the effects of climate change on water yield and forest production in the northeastern U.S. Climate Research 5:207–222.

Askne, J., M. Santoro, G. Smith, and J. E. S. Fransson. 2003. Multitemporal repeat-pass SAR interferometry of boreal forests. IEEE Transactions on Geoscience and Remote Sensing 41(7):1540–1550.

Asner, G. P., C. Borghi, and R. Ojeda. 2003. Desertification in Central Argentina: Regional changes in ecosystem carbon-nitrogen from imaging spectroscopy. Ecological Applications 13:629–648.

Bergen, K. M., and M. C. Dobson. 1999. Integration of remotely sensed radar imagery in modeling and mapping of forest biomass and net primary production. Ecological Modelling 122:257–274.

Blair, J. B., D. L. Rabine, and M. A. Hofton. 1999. The Laser Vegetation Imaging Sensor (LVIS): A medium-altitude, digitisation-only, airborne laser altimeter for mapping vegetation and topography. ISPRS Journal of Photogrammetry and Remote Sensing 54:115–122.

Braswell, B. H., D. S. Schimel, E. Linder, and B. Moore. 1997. The response of global terrestrial ecosystems to interannual temperature variability. Science 238:870–872.

Cohen, W. B., and C. O. Justice. 1999. Validating MODIS terrestrial ecology products: Linking in situ and satellite measurements. Remote Sensing of Environment 70(1): 1–3.

Cohen W. B., T. K. Maiersperger, S. T. Gower, and D. P. Turner. 2003. An improved strategy for regression of biophysical variables and Landsat ETM+ data. Remote Sensing of Environment 84(4): 561–571.

Comins, H. N., and R. E. McMurtrie. 1993. Long-term response of nutrient-limited forests to CO_2-enrichment: Equilibrium behaviour of plant-soil models. Ecological Applications 3:666–681.

Dobson, M. C., F. T. Ulaby, L. E. Pierce, T. L. Sharik, K. M. Bergen, J. Kellndorfer, J. R. Kendra, E. Li , C. Lin, A. Nashashibi, K. Sarabandi, and P. Siqueira. 1995. Estimation of forest biophysical characteristics in Northern Michigan with SIR-C/X-SAR. IEEE Transactions on Geoscience and Remote Sensing 33(4):877–892.

Drake, J. B., R. O. Dubayah, D. B. Clark, R. G. Knox, J. B. Blair, M. A. Hofton, R. L. Chazdon, J. F. Weishampel, and S. D. Prince. 2002. Estimation of tropical forest structural characteristics using large-footprint lidar. Remote Sensing of Environment 79: 305–319.

Drake, J. B., R. G. Knox, R. O. Dubayah, D. B. Clark, R. Condit, J. B. Blair, and M. Hofton. 2003. Above-ground biomass estimation in closed canopy neotropical forests using lidar remote sensing: Factors affecting the generality of relationships. Global Ecology and Biogeography 12:147–159.

Dubayah, R. O., and J. B. Drake. 2000. Lidar remote sensing for forestry. Journal of Forestry 98:44–46.

Ehleringer, J. R., and C. B. Field (eds.). 1993. Scaling Physiological Processes: Leaf to Globe. Academic Press, San Diego.

Fahey, T. J., T. G. Siccama, C. T. Driscoll, G. E. Likens, J. Campbell, C. E. Johnson, J. D. Aber, J. J. Cole, M. C. Fisk, P. M. Groffman, S. P. Hamburg, R. T. Holmes, P. A. Schwarz, and R. D. Yanai. 2005. The biogeochemistry of carbon at Hubbard Brook. Biogeochemistry 75 (1): 109–176.

Fassnacht, K. S., and S. T. Gower. 1997. Interrelationships among the edaphic and stand characteristics, leaf area index, and aboveground net primary production of upland forest ecosystems in north central Wisconsin. Canadian Journal of Forest Research 27:1058–1067.

Ferrazzoli, P., S. Paloscia, P. Pampaloni, G. Schiavon, S. Sigismondi, and D. Solimini. 1997. The potential of multifrequency polarimetric SAR in assessing agricultural and arboreous biomass. IEEE Transactions on Geoscience and Remote Sensing 35(1):5–17.

Field, C. 1991. Ecological scaling of carbon gain to stress and resource availability. Pages 35–65 in H. A. Mooney, W. E. Winner, and E. J. Pell (eds.), Response of Plants to Multiple Stresses. Academic Press, San Diego.

Field, C., and H. A. Mooney. 1986. The photosynthesis-nitrogen relationship in wild plants. Pages 25–55 in T. J. Garvish (ed.), On the Economy of Plant Form and Function. Cambridge University Press, Cambridge.

Flood, M. 2001. Lidar activities and research priorities in the commerical sector. Pages 3–7 in Hofton, M.A. (ed), Land Surface Mapping and Characterization Using Laser Altimetry. International Archives of Photogrammetry, Remote Sensing, and Spatial Information Sciences. Vol XXXIV-3/W4. ISPRS Workshop. Annapolis, MD. 22–24 Oct. 2001.

Friedl, M. A., D. K. McIver, J. C. F. Hodges, X. Y. Zhang, D. Muchoney, A. H. Strahler, C. E. Woodcock, S. Gopal, A. Schneider, A. Cooper, A. Baccini, F. Gao, and C. Schaaf. 2002. Global land cover mapping from MODIS: Algorithms and early results. Remote Sensing of Environment 83(1–2):287–302.

Fuentes, D. A., J. A. Gamon, H.-L. Qiu, D. A. Sims, and D. A. Roberts. 2001. Mapping Canadian boreal forest vegetation using pigment and water absorption features derived from the AVIRIS sensor. Journal of Geophysical Research 106:33565–33577.

Gower, S. T., C. J. Kucharik, and J. M. Norman. 1999. Direct and indirect estimation of leaf area index, f(APAR), and net primary production of terrestrial ecosystems. Remote Sensing of Environment 70(1):29–51.

Gower, S. T., P. B. Reich, and Y. Son. 1993. Canopy dynamics and aboveground production of five tree species with different leaf longevities. Tree Physiology 12(4): 327–345.

Gower, S. T., K. A. Vogt, and C. C. Grier. 1992. Carbon dynamics of Rocky Mountain Douglas fir: Influence of water and nutrient availability. Ecological Monographs 62:43–65.

Green, D. S., J. E. Erickson, and E. L. Kruger. 2003. Foliar morphology and canopy nitrogen as predictors of light-use efficiency in terrestrial vegetation. Agricultural and Forest Meteorology 3097:1–9.

Harding, D. J., M. A. Lefsky, G. G. Parker, and J. B. Blair. 2001. Laser altimeter canopy height profiles. Methods and validation for closed-canopy, broadleaf forests. Remote Sensing of Environment 76:283–297.

Haxeltine, A., and I. C. Prentice. 1996. A general model for the light-use efficiency of primary production. Functional Ecology 10:551–561.

Hirose, T., and M. J. A. Werger. 1987. Maximizing daily canopy photosynthesis with respect to the leaf nitrogen allocation pattern in the canopy. Oecologia 72:520–526.

Hofton, M. A., J. B. Minster, and J. B. Blair. 2000. Decomposition of laser altimeter waveforms. IEEE Transactions on Geoscience and Remote Sensing 38:1989–1996.

Hollinger, D. Y. 1989. Canopy organization and foliage photosynthetic capacity in a broad-leaved evergreen montane forest. Functional Ecology 3:53–62.

Hurtt, G. C., R. Dubayah, J. Drake, P. Moorcroft, S. W. Pacala, J. B. Blair, and M. G. Fearon. 2004. Beyond potential vegetation: Combining lidar data and a height-structured model for carbon studies. Ecological Applications 14:873–883.

Imhoff, M. L. 1995. A theoretical analysis of the effect of forest structure on synthetic aperture radar backscatter and the remote sensing of biomass. IEEE Transactions on Geoscience and Remote Sensing 33(2):341–352.

Jacquemoud, S., and F. Baret. 1990. PROSPECT: A model of leaf optical properties spectra. Remote Sensing of Environment 34:75–91.

Kellndorfer, J., W. Walker, L. Pierce, C. Dobson, J. A. Fites, C. Hunsaker, J. Vona, and M. Clutter. 2004. Vegetation height estimation from shuttle radar topography mission and national elevation datasets. Remote Sensing of Environment 93(3):339–358.

Kicklighter, D. W., A. Bondeau, A. L. Schloss, J. Kaduk, and A. D. McGuire. 1999. Comparing global models of terrestrial net primary productivity (NPP): Global pattern and differentiation by major biomes. Global Change Biology 5(suppl. 1):16–24.

Kimball, J. S., A. R. Keyser, S. W. Running, and S. S. Saatchi. 2000. Regional assessment of boreal forest productivity using an ecological process model and remote sensing parameter maps. Tree Physiology 20(11):761–775.

Kotchenova, Y. S., X. Song, N. V. Shabanov, C. S. Potter, Y. Knyazikhin, and R. B. Myneni. 2004. Lidar remote sensing for modeling gross primary production of deciduous forests. Remote Sensing of Environment 92:158–172.

Lefsky, M. A., W. B. Cohen, S. A. Acker, G. Parker, T. A. Spies, and D. Harding. 1999a. Lidar remote sensing of the canopy structure and biophysical properties of Douglas fir-western hemlock forests. Remote Sensing of Environment 70:339–361.

Lefsky, M. A., W. B. Cohen, D. J. Harding, G. G. Parker, S. A. Acker, and S. T. Gower. 2002a. Lidar remote sensing of aboveground biomass in three biomes. Global Ecology and Biogeography 11:393–399.

Lefsky, M. A., W. B. Cohen, G. G. Parker, and D. J. Harding. 2002b. Lidar remote sensing for ecosystem studies. Bioscience 52(1):19–30.

Lefsky, M. A., W. B. Cohen, and T. A. Spies. 2001. An evaluation of alternate remote sensing products for forest inventory, monitoring, and mapping of Douglas-fir forests in western Oregon. Canadian Journal of Forest Research 31:78–87.

Lefsky, M. A., D. Harding, W. B. Cohen, G. Parker, and H. H. Shugart. 1999b. Surface lidar remote sensing of basal area and biomass in deciduous forest of eastern Maryland, USA. Remote Sensing of Environment 67:83–98.

Lefsky, M. A., A. T Hudak, W. B. Cohen, and S. A. Acker. 2005a. Geographic variability in lidar predictions of forest stand structure in the Pacific Northwest. Remote Sensing of Environment 95:532–548.

Lefsky, M. A., D. P. Turner, M. Guzy, and W. B. Cohen. 2005b. Combining lidar estimates of above ground biomass and Landsat estimates of stand age for spatially extensive validation of modeled forest productivity. Remote Sensing of Environment 95: 549–558.

Lim, K., P. Treitz, M. Wulder, B. St-Onge, and M. Flood. 2003. Lidar remote sensing of forest structure. Progress in Physical Geography 27(1):88–106.

Liu, J., J. M. Chen, J. Cihlar, and W. Chen. 1999. Net primary productivity distribution in the BOREAS region from a process model using satellite and surface data. Journal of Geophysical Research—Atmospheres 104:27735–27754.

Luckman, A., J. Baker, M. Honzák, and R. Lucas. 1998. Tropical forest biomass density estimation using JERS-1 SAR: Seasonal variation, confidence limits, and application to image mosaics. Remote Sensing of Environment 63:126–139.

Luckman, A., J. Baker, and U. Wegmüller. 2000. Repeat-pass interferometric coherence measurements of disturbed tropical forest from JERS and ERS satellites. Remote Sensing of Environment 73:350–360.

Luo, T. X., Y. D. Pan, H. Ouyang, P. L. Shi, J. Luo, Z. L. Yu, and Q. Lu. 2004. Leaf area index and net primary productivity along subtropical to alpine gradients in the Tibetan Plateau. Global Ecology and Biogeography 13(4):345–358.

Magnussen, S., and P. Boudewyn. 1998. Derivations of stand heights from airborne laser scanner data with canopy-based quantile estimators. Canadian Journal of Forest Research 28(7):1016–1031.

Marion, J. B. 1965. Classical Electromagnetic Radiation. Academic Press, New York.

Martin, M. E., and J. D. Aber. 1997. Estimation of forest canopy lignin and nitrogen concentration and ecosystem processes by high spectral resolution remote sensing. Ecological Applications 7:441–443.

Martin, M. E., S. D. Newman, J. D. Aber, and R. G. Congalton. 1998. Determining forest species composition using high spectral resolution remote sensing data. Remote Sensing of Environment 65:249–254.

Matson, P., L. Johnson, C. Billow, J. Miller, and R. Pu. 1994. Seasonal patterns and remote spectral estimation of canopy chemistry across the Oregon transect. Ecological Applications 4(2):280–298.

Means, J. E., S. A. Acker, D. J. Harding, J. B. Blair, M. A. Lefsky, W. B. Cohen, M. E. Harmon, and W. A. McKee. 1999. Use of large-footprint scanning airborne lidar to estimate forest stand characteristics in the Western Cascades of Oregon. Remote Sensing of Environment 67:298–308.

Mencuccini, M., and J. Grace. 1996. Hydraulic conductance, light interception and needle nutrient concentration in Scots pine stands and their relations with net primary productivity. Tree Physiology 16:459–468.

Monteith, J. L. 1972. Solar radiation and productivity in tropical ecosystems. Applied Ecology 9:747–766.

Moorcroft, P. R., G. C. Hurtt, and S. W. Pacala. 2001. A method for scaling vegetation dynamics: The ecosystem demography model (ED). Ecological Monographs 71:557–585.

Moreau, S., and T. Le Toan. 2003. Biomass quantification of Andean wetland forages using ERS satellite SAR data for optimizing livestock management. Remote Sensing of Environment 84:477–492.

Myneni, R. B., and D. L. Williams. 1994. On the relationship between FAPAR and NDVI. Remote Sensing of Environment 49:200–211.

Naesset, E. 2002. Predicting forest stand characteristics with airborne scanning laser using a practical two-stage procedure and field data. Remote Sensing of Environment 80:88–99.

Naesset, E. 2004. Effects of different flying altitudes on biophysical stand properties estimated from canopy height and density measured with a small footprint airborne scanning laser. Remote Sensing of Environment 91:243–255.

Nelson, R., M. A. Valenti, A. Short, and C. Keller. 2003. A multiple resource inventory of Delaware using airborne laser data. Bioscience 53:981–992.

Nilsson, M. 1996. Estimation of tree heights and stand volume using an airborne lidar system. Remote Sensing of Environment 56:1–7.

Ollinger, S. V., J. D. Aber, and C. A. Federer. 1998. Estimating regional forest productivity and water balances using an ecosystem model linked to a GIS. Landscape Ecology 13(5):323–334.

Ollinger, S. V., and M. L. Smith. 2005. Net primary production and canopy nitrogen in a

considerations for operational monitoring. International Journal of Remote Sensing 23 (7):1381–1399.

Santoro, M., J. Askne, G. Smith, and J. E. S. Fransson. 2002. Stem volume retrieval in boreal forests from ERS-1/2 interferometry. Remote Sensing of Environment 81:19–35.

Santos, J. R., C. C. Freitas, L. S. Araujo, L. V. Dutra, J. C. Mura, F. F. Gama, L. S. Soler, and S. J. S. Sant'Anna. 2003. Airborne P-band SAR applied to the aboveground biomass studies in the Brazilian tropical rain forest. Remote Sensing of Environment 87: 482–493.

Sellers, P. J. 1987. Canopy reflectance, photosynthesis, and transpiration. II: The role of biophysics in the linearity of their interdependence. International Journal of Remote Sensing 6:1335–1372.

Sellers, P. J., J. A. Berry, G. J. Collatz, C. B. Field, and F. G. Hall. 1992. Canopy reflectance, photosynthesis, and transpiration. III. A reanalysis using improved leaf models and a new canopy integration scheme. Remote Sensing of Environment 42: 187–216.

Smith, G., L. M. H. Ulander and J. Askne. 1999. VHF Backscatter Sensitivity to Forest Properties: Model Predictions. Geoscience and Remote Sensing Symposium, 1999. IGARSS '99 Proceedings. IEEE 1999 International 4: 1889–1891.

Smith, M. L., S. V. Ollinger, M. E. Martin, J. D. Aber, and C. L. Goodale. 2002. Direct prediction of aboveground forest productivity by remote sensing of canopy nitrogen. Ecological Applications 12(5):1286–1302.

Townsend, P. A., J. R. Foster, and R. A. Chastain, Jr. 2003. Imaging spectroscopy and canopy nitrogen: Application to the forests of the central Appalachian Mountains using Hyperion and AVIRIS. IEEE Transactions on Geoscience and Remote Sensing 41(6): 1347–1354.

Treuhaft, R. N., G. P. Asner, and B. E. Law. 2003. Structure-based forest biomass from fusion of radar and hyperspectral observations. Geophysical Research Letters 30: 1472–1475.

Treuhaft, R. N., B. E. Law, and G. P. Asner. 2004. Forest attributes from radar interferometric structure and its fusion with optical remote sensing. BioScience 54(6): 561–571.

Treuhaft, R. N., S. N. Madsen, M. Moghaddam, and J. J. Van Zyl. 1996. Vegetation characteristics and surface topography from interferometric radar. Radio Science 31: 1449–1485.

Treuhaft, R. N., and P. R. Siqueira. 2004. The calculated performance of forest structure and biomass from interferometric radar. Waves in Random Media 14(2):S345–S358.

Tucker, C. J. 1979. Red and photographic infrared linear combinations for monitoring vegetation. Remote Sensing of Environment 8:27–150.

Turner, D. P., W. B. Cohen, R. E. Kennedy, K. S. Fassnacht, and J. M. Briggs. 1999. Relationships between leaf area index and Landsat TM spectral vegetation indices across three temperate zone sites. Remote Sensing of Environment 70:52–68.

Turner, D. P., S. V. Ollinger, and J. S. Kimball. 2004. Integrating remote sensing and ecosystem process models for landscape to regional scale analysis of the carbon cycle. BioScience 54:573–584.

Turner, D. P., S. Ollinger, M. L. Smith, O. Krankina, and M. Gregory. 2003a. Scaling net primary production to a MODIS footprint in support of Earth observing system product validation. International Journal of Remote Sensing 25:1961–1979.

Turner, D. P., W. D. Ritts, W. B. Cohen, S. T. Gower, M. Zhao, S. W. Running, S. C. Wofsy, S. Urbanski, A. Dunn, and J. W. Munger. 2003b. Scaling gross primary production (GPP) over boreal and deciduous forest landscapes in support of MODIS GPP product validation. Remote Sensing of Environment 88:256–270.

Ustin, S. L., D. A. Roberts, J. A. Gamon, G. P. Asner, and R. O. Green. 2004. Using imaging spectroscopy to study ecosystem processes and properties. Bioscience 54(6): 523–534.

Verhoef, W. 1984. Light scattering by leaf layers with application to canopy reflectance modeling: The SAIL model. Remote Sensing of Environment 16:125–141.

Vose, J. M., and H. L. Allen. 1988. Leaf area, stemwood growth and nutritional relationships in loblolly pine. Forest Science 34:547–563.

Wagner, W., A. Luckman, J. Vietmeier, K. Tansey, H. Balzter, C. Schmullius, M. Davidson, D. Gaveau, M. Gluck, T. Le Toan, S. Quegan, A. Shvidenko, A. Wiesmann, and J. J. Yu. 2003. Large-scale mapping of boreal forest in Siberia using ERS tandem coherence and JERS backscatter data. Remote Sensing of Environment 85: 125–144.

Waring, R. H., and S. W. Running. 1998. Forest Ecosystems: Analysis at Multiple Scales. San Diego, Academic Press.

Webb, W. L., W. Lauenroth, S. R. Szarek, and R. S. Kinerson. 1983. Primary production and abiotic controls in forests, grasslands, and desert ecosystems in the United States. Ecology 64(1):134–151.

Wehr, A., and U. Lohr. 1999. Airborne laser scanning—an introduction and overview. ISPRS Journal of Photogrammetry and Remote Sensing 54:68–82.

Xiao, X., D. Y. Hollinger, J. D. Aber, M. Goltz, E. A. Davidson, Q. Zhang, and B. Moore. 2004. Satellite-based modeling of gross primary productivity in an evergreen needleleaf forest. Remote Sensing of Environment 89:519–534.

Yin, X. W. 1993. Variation in foliar nitrogen concentration by forest type and climatic gradients in North America. Canadian Journal of Forest Research 23(8):1587–1602.

Yoder, B. J., and R. E. Pettigrew-Crosby. 1995. Predicting nitrogen and chlorophyll content and concentrations from reflectance spectra (400–2500 nm) at leaf and canopy scales. Remote Sensing of Environment 53:199–211.

Zagloski, F., V. Pinel, et al. 1996. Forest canopy chemistry with high spectral resolution remote sensing. International Journal of Remote Sensing 17:1107–1128.

Zwally, H. J., B. Schutz, W. Abdalati, J. Abshire, C. Bentley, A. Brenner, J. Bufton, J. Dezio, D. Hancock, D. Harding, T. Herring, B. Minster, K. Quinn, S. Palm, J. Spinhirne, and R. Thomas. 2002. ICESat's laser measurements of polar ice, atmosphere, ocean and land. Journal of Geodynamics 34:405–445.